



AFRL-RY-WP-TP-2008-1152

**SYMMETRIC PHASE-ONLY MATCHED FILTER (SPOMF)
FOR FREQUENCY-DOMAIN SOFTWARE GNSS
RECEIVERS (POSTPRINT)**

**Chun Yang, Mikel Miller, and Thao Nguyen
Sigtem Technology, Inc.**

SEPTEMBER 2006

Approved for public release; distribution unlimited.

See additional restrictions described on inside pages

STINFO COPY

© 2006 IEEE

**AIR FORCE RESEARCH LABORATORY
SENSORS DIRECTORATE
WRIGHT-PATTERSON AIR FORCE BASE, OH 45433-7320
AIR FORCE MATERIEL COMMAND
UNITED STATES AIR FORCE**

REPORT DOCUMENTATION PAGE				<i>Form Approved</i> OMB No. 0704-0188	
<p>The public reporting burden for this collection of information is estimated to average 1 hour per response, including the time for reviewing instructions, searching existing data sources, gathering and maintaining the data needed, and completing and reviewing the collection of information. Send comments regarding this burden estimate or any other aspect of this collection of information, including suggestions for reducing this burden, to Department of Defense, Washington Headquarters Services, Directorate for Information Operations and Reports (0704-0188), 1215 Jefferson Davis Highway, Suite 1204, Arlington, VA 22202-4302. Respondents should be aware that notwithstanding any other provision of law, no person shall be subject to any penalty for failing to comply with a collection of information if it does not display a currently valid OMB control number. PLEASE DO NOT RETURN YOUR FORM TO THE ABOVE ADDRESS.</p>					
1. REPORT DATE (DD-MM-YY) September 2006		2. REPORT TYPE Conference Paper Postprint		3. DATES COVERED (From - To) 08 April 2005 – 08 September 2006	
4. TITLE AND SUBTITLE SYMMETRIC PHASE-ONLY MATCHED FILTER (SPOMF) FOR FREQUENCY-DOMAIN SOFTWARE GNSS RECEIVERS (POSTPRINT)				5a. CONTRACT NUMBER FA8650-05-C-1828	
				5b. GRANT NUMBER	
				5c. PROGRAM ELEMENT NUMBER 65502F	
6. AUTHOR(S) Chun Yang (Sigtem Technology, Inc.) Mikel Miller and Thao Nguyen (AFRL/RYRN)				5d. PROJECT NUMBER 3005	
				5e. TASK NUMBER 13	
				5f. WORK UNIT NUMBER 300513CY	
7. PERFORMING ORGANIZATION NAME(S) AND ADDRESS(ES) Sigtem Technology, Inc. 113 Clover Hill Lane Harleysville, PA 19438-1693				8. PERFORMING ORGANIZATION REPORT NUMBER	
Reference Systems Branch (AFRL/RYRN) RF Sensor Technology Division Air Force Research Laboratory, Sensors Directorate Wright-Patterson Air Force Base, OH 45433-7320 Air Force Materiel Command, United States Air Force					
9. SPONSORING/MONITORING AGENCY NAME(S) AND ADDRESS(ES) Air Force Research Laboratory Sensors Directorate Wright-Patterson Air Force Base, OH 45433-7320 Air Force Materiel Command United States Air Force				10. SPONSORING/MONITORING AGENCY ACRONYM(S) AFRL/RYRN	
				11. SPONSORING/MONITORING AGENCY REPORT NUMBER(S) AFRL-RY-WP-TP-2008-1152	
12. DISTRIBUTION/AVAILABILITY STATEMENT Approved for public release; distribution unlimited.					
13. SUPPLEMENTARY NOTES Paper produced under contract FA8650-05-C-1828 for technical report AFRL-RY-WP-TR-2008-1137, SOFTWARE TOOLKIT FOR NONLINEAR FILTERS FOR GLOBAL POSITIONING SYSTEM (GPS) OPERATIONAL CONTROL SEGMENT (OCS) ESTIMATION AND OTHER APPLICATIONS. Conference paper published in the Proceedings of the IEEE PLANS, Position Location and Navigation Symposium, 2006 (conference held Apr 25-27 2006, San Diego, CA; Publisher: Institute of Electrical and Electronics Engineers Inc.). © 2006 IEEE. The U.S. Government is joint author of this work and has the right to use, modify, reproduce, release, perform, display, or disclose the work. PAO Case Number: SN 06-0061; Clearance date: 23 Feb 2006. Paper contains color.					
14. ABSTRACT As a powerful tool, the symmetric phase-only matched filter (SPOMF) has been shown to yield superior performance over the conventional correlator and is widely used in image registration and recognition. In this paper, we investigate the use of this SPOMF for processing GNSS signals. This extension is compatible with our frequency-domain software GNSS receiver architecture in which both the incoming signal and replica spectra are available for the SPOMF implementation versus the conventional correlator. <p style="text-align: right;"><i>Abstract concludes on reverse side →</i></p>					
15. SUBJECT TERMS					
16. SECURITY CLASSIFICATION OF:			17. LIMITATION OF ABSTRACT: SAR	18. NUMBER OF PAGES 18	19a. NAME OF RESPONSIBLE PERSON (Monitor) Thao Nguyen 19b. TELEPHONE NUMBER (Include Area Code) N/A
a. REPORT Unclassified	b. ABSTRACT Unclassified	c. THIS PAGE Unclassified			

14. ABSTRACT (concluded)

The use of phase-only information is equivalent to equalizing the magnitude spectrum in contrast to the original spectrum that tapers off according to a sinc-function. This tends to accentuate the high frequency components corresponding to edges or transitions in the signals. As such, the SPOMF produces a much sharper peak (ideally a Dirac delta function) that is more accurate in timing and less sensitive to multipath. In addition, the same operation is applicable to both a binary phase shift keying (BPSK) modulated signal such as the GPS C/A-code and P-code and a binary offset carrier (BOC) modulation such as the GPS M-code and Galileo codes. More importantly, it only has a single matching peak regardless of which modulation code is being used.

In this paper, the SPOMF is introduced within the framework of a generalized frequency-domain correlator (GFDC) for GNSS signals. The salient features of SPOMF as well as its application to BPSK and BOC signals are illustrated with simulation examples.

Symmetric Phase-Only Matched Filter (SPOMF) for Frequency-Domain Software GNSS Receivers

Mikel Miller

Air Force Research Lab/SNRN
2241 Avionics Circle, Bldg 620
WPAFB, OH 45433-7301
mikel.miller@wpafb.af.mil

Thao Nguyen

Air Force Research Lab/SNRN
2241 Avionics Circle, Bldg 620
WPAFB, OH 45433-7301
thao.nguyen@wpafb.af.mil

Chun Yang

Sigtem Technology, Inc.
113 Clover Hill Lane
Harleysville, PA 19438-1693
chunyang@sigtem.com

Abstract—As a powerful tool, the symmetric phase-only matched filter (SPOMF) has been shown to yield superior performance over the conventional correlator and is widely used in image registration and recognition. In this paper, we investigate the use of this SPOMF for processing GNSS signals. This extension is compatible with our frequency-domain software GNSS receiver architecture in which both the incoming signal and replica spectra are available for the SPOMF implementation versus the conventional correlator.

The use of phase-only information is equivalent to equalizing the magnitude spectrum in contrast to the original spectrum that tapers off according to a *sinc*-function. This tends to accentuate the high frequency components corresponding to edges or transitions in the signals. As such, the SPOMF produces a much sharper peak (ideally a Dirac delta function) that is more accurate in timing and less sensitive to multipath. In addition, the same operation is applicable to both a binary phase shift keying (BPSK) modulated signal such as the GPS C/A-code and P-code and a binary offset carrier (BOC) modulation such as the GPS M-code and Galileo codes. More importantly, it only has a single matching peak regardless of which modulation code is being used.

In this paper, the SPOMF is introduced within the framework of a generalized frequency-domain correlator (GFDC) for GNSS signals. The salient features of SPOMF as well as its application to BPSK and BOC signals are illustrated with simulation examples.

I. INTRODUCTION

Correlation is a critical operation in GPS receivers. As a spread-spectrum signal, the received GPS signal is below the thermal noise. Through despreading integration, correlation provides the processing gain necessary to detect a signal from noise and by doing so, it identifies which satellite the acquired signal is coming from. Correlations with code and carrier replicas at different code phases and carrier phases provide code delay errors and carrier phase/frequency errors that are used as input to code and carrier tracking loops, respectively. The accumulated correlations are further used for navigation data bit sync and demodulation. These and other pieces of information lead to GPS observables and satellite ephemerides for the ultimate timing and position fixing [5, 7, 10, 12].

For a maximum-length pseudo-random number (PRN) code, its correlation function is ideally an equilateral triangle with its base width being $\pm T_c$ where $T_c = 1/f_c$ is the chip

duration and f_c is the chipping rate. In the acquisition mode, the search step in code phase is typically chosen as $\Delta t = T_c/2$ and this produces the worst signal loss of 2.5 dB. It is therefore desirable to have a correlation function with a wide base in the acquisition mode so that a minimal number of steps are needed to cover a given interval of time uncertainty. That was one reason for which the GPS C/A-code (i.e., the coarse acquisition code) was originally designed so as to assist the precision P-code.

In the tracking mode, however, it is desired to have a correlation function with its base as narrow as possible. Such a sharp correlation function not only provides more precise timing but also results in a delay estimate that is less sensitive to multipath. This is due to the fact that only very closely spaced multipath signals ($< 1.5T_c$) can contribute to the delay estimation errors and at much closer ranges the errors are insignificant as compared to thermal noise.

Clearly different requirements are imposed on correlation function for acquisition and tracking, which are in conflict. A code that may satisfy both requirements at the same time is the binary offset carrier (BOC) modulation as used by the new M-code and LIC-code (under development) as well as the European Galileo codes. By placing the signal power toward the edges of the frequency band, it was designed to co-exist with binary phase shift keying (BPSK)-codes already in the same band with reduced interference since a BPSK code power is concentrated around the band center. The PRN code of a BOC modulation has a correlation function with a large base that can be obtained with a single sideband (either upper or lower) [16, 17]. Together with the offsetting square wave, the composite correlation of a BOC code has a refined mainlobe. However, it also has numerous nulls and sidelobes. Although the mainlobe is narrow, the sidelobes are not substantially smaller. Without special hardware and software, a receiver runs the risk of being trapped in nulls (i.e., missing detection) or locking onto a sidelobe (i.e., biased measurements) [1, 3].

In this paper, we set forth a generalized frequency-domain correlator (GFDC) to satisfy the correlation function requirements in both the acquisition and tracking modes for BPSK- and BOC-types of codes alike. The refined correlation

Research supported in part under Contract No. FA8650-05-C-1828, which is gratefully acknowledged.

function is obtained by implementing the symmetric phase-only matched filter (SPOMF) in the tracking mode while a conventional correlator is implemented in the acquisition mode (with single sideband segmentation for the BOC codes for instance [16]).

The SPOMF is widely used in image registration and recognition [2, 9, 13] and its extension to GNSS signal processing is compatible with our frequency-domain GNSS software receiver architecture [15] in which both the incoming signal and replica spectra are available for flexible implementation. In this paper, the SPOMF is introduced within the framework of GFDC for GNSS signals. The salient features of SPOMF as well as its application to BPSK and BOC signals are illustrated with simulation examples.

II. GENERALIZED FREQUENCY-DOMAIN CORRELATOR (GFDC)

We will introduce the symmetric phase-only matched filter (SPOMF) as a particular implementation of the generalized frequency-domain correlator (GFDC), as part of a frequency-domain software GNSS receiver. However, it can be used standalone or as a replacement of conventional correlators in conventional GPS receivers.

The inherent flexibility of a software GPS receiver allows it to adopt a frequency-domain baseband processor for which a GFDC is shown in Fig. 1. The use of a GFDC has several advantages. First, the same operation is applicable, without any other changes except for the replica code, to both the BPSK codes such as GPS C/A-code and the BOC modulations such as M-code. Second, it can switch seamlessly among different types of correlation/matching operations with the wide base for acquisition and narrow base for tracking. Third, the generalized correlation has a sharp peak when the SPOMF is in use. The reduced base width makes it more accurate in timing and less sensitive to multipath.

This GFDC differs from the generalized cross correlator (GCC) that has been used for radar and sonar signal processing for delay estimation [4, 6]. The GCC is closely related to the coherence, a complex quantity that is the cross-power spectral density between two random processes divided by the product of their auto power spectral densities. The design goal of the GCC is to produce the highest signal-to-noise ratio (SNR) correlation peaks in the presence of noise. The optimum filter is designed with the spectral characteristics of the noise assumed to be known. However, some of these filters alter the phase of the input functions, which could bias the final output [13].

As shown in Fig. 1, the GFDC accepts the incoming signal $s(t)$ and the code replica $r(t)$ and produces the correlation function $c(t)$ between the two. This is the same input-output behavior as other correlators. However, what makes it different from others is the spectrum filtering $U(f)$, $V(f)$, and $W(f)$ applied along the signal processing chain and the feedback paths inserted in the frequency domain.

Clearly, when $U(f) = 1$, $V(f) = 1$, and $W(f) = 1$ (i.e., without any spectrum manipulation and feedback), it becomes a simple straight FFT-implemented correlation.

Various spectrum filtering can be applied that makes the GFDC design versatile, which is discussed below.

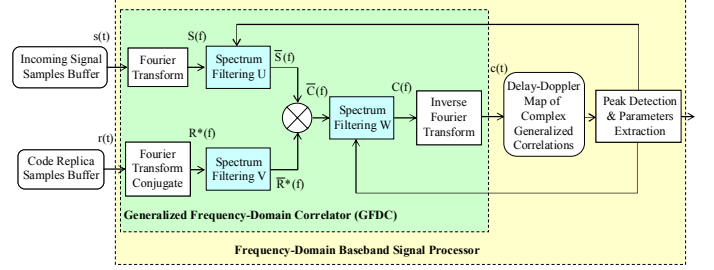


Fig. 1. Generalized Frequency-Domain Correlator (GFDC) Architecture

A. Incoming Signal Spectrum Filtering and Feedback

A number of spectrum filtering techniques applicable to the incoming signal are described below. They do not serve the same purposes and not all are applicable at the same time.

(a) *Spectrum Excision of Narrowband Interference.* Being spread-spectrum, the GPS signal is below the thermal noise. Any spikes in the signal spectrum are attributed to interference and as such, the spectrum values at those frequency bins can be removed and replaced with zeros. This requires continuous monitoring of the spectrum and power-detection against a pre-defined threshold [19]. The operation of excision can be viewed as passing the signal through a notch filter in the time domain or equivalently as multiplying the spectrum with zero at those frequency bins of interference. Assume there are N frequency bins. The N spectrum complex values can be put into a vector as $\underline{S} = [S(f), f = 0, 1, \dots, N-1]^T$, where the superscript T stands for transpose. To remove an interference component at the k^{th} frequency bin, the following operation is applied:

$$\underline{S}_k = Z_k \underline{S} \quad (1a)$$

$$Z_k = \text{diag}(\underline{1}_{k-1} \quad 0 \quad \underline{1}_{N-k}) \quad (1b)$$

where $\text{diag}(\underline{v})$ stands for a diagonal matrix with its diagonal elements specified by \underline{v} and $\underline{1}_n$ is a vector of n ones (1's). The operation can be repeated for all frequency bins of interest. It is implied that the same operation is applied to both corresponding positive and negative frequency bins at the same time. Zone-zeroing and individual excision are two popular ways to apply this spectral filtering.

(b) *Spectral Filtering to Reduce Additive Noise.* To restore the signals under additive noise, the following spectral filter can be applied:

$$U(f) = \left[\frac{P_s(f)}{P_s(f) + \alpha P_n(f)} \right]^\beta \quad (2a)$$

where $P_s(f)$ and $P_n(f)$ represent the power spectrum of the signal and the additive noise, respectively. When $\alpha = \beta = 1$, Eq. (2) corresponds to Wiener filtering. When $\alpha = 1$ and $\beta = 1/2$, it applies power spectrum filtering. It is clear from Eq. (2) that the filter is non-causal with an even, real frequency

response and consequently the phase of the filter is zero. This filter does not affect the signal phase but does modify the magnitude.

When the signal plus noise power spectrum is estimated from the observed samples, denoted by $\hat{P}_{sn}(f)$, Eq. (2a) can be modified as:

$$U(f) = \frac{1}{\hat{P}_{sn}(f)} \quad (2b)$$

This spectral filter can be used to suppress narrowband interference [11].

(c) *Spectrum Segmentation of Multiple Codes.* In the case where each GPS signal band (L1, L2, or L5) is processed, the spectrum for individual codes need to be extracted from the full band spectrum [16]. The operation can be viewed as passing the signal through a bandpass filter in the time domain or equivalently as selecting the spectrum at those frequency bins of interest. Both are linear operations. Assume we want to segment the spectrum at frequency bins from i to j . The following matrix multiplication implements an ideal bandpass filtering:

$$\underline{S}_i^j = G_i^j \underline{S} \quad (3a)$$

$$G_i^j = \text{diag}(\underline{0}_{i-1}, \underline{1}_{j-i+1}, \underline{0}_{N-j}) \quad (3b)$$

where $\underline{0}_n$ is a vector of n zeros (0 's).

(d) *Spectrum Translation for Residual Doppler Removal with Feedback.* The residual Doppler in the incoming signal appears as a multiplicative sine or cosine term to the code sequence, thus introducing a phase change from sample to sample. It is typically removed by multiplying the incoming signal with a carrier replica in the form of complex exponential at the desired Doppler frequency. This time-domain phase rotation is equivalent to spectrum translation in the frequency domain [19]. To remove a residual Doppler of $\pm d\Delta f$ Hz where Δf is the frequency resolution (i.e., the width of each frequency bin), the spectrum is down (up)-translated by d bins.

$$\underline{S}_d = T_d \underline{S} \quad (4a)$$

$$T_{d=0} = I \quad (4b)$$

$$T_{d \neq 0} = \begin{bmatrix} 0 & \underline{0}_{d-2} & 1 & \underline{0}_{N-d} \\ \vdots & \vdots & \vdots & \vdots \\ 0 & \underline{0}_{N-3} & 0 & 1 \\ 1 & 0 & \underline{0}_{N-3} & 0 \\ \vdots & \vdots & \vdots & \vdots \\ \underline{0}_{d-2} & 1 & 0 & \underline{0}_{N-d} \end{bmatrix} \quad (4c)$$

where the first non-zero element in the first row is at the d^{th} column when $d > 0$ and at the $(N+d)^{\text{th}}$ column when $d < 0$, with N being the number of frequency bins. Since the matrix multiplication in Eq. (4a) is equivalent to index permutation, the practical implementation resorts to circularly shifted indexing of the array.

Without knowing the residual Doppler frequency, the initial search will select a large value for d so as to cover the

frequency uncertainty interval. However, in the tracking mode, the estimated Doppler and its uncertainty will reduce it to a small interval, say, from d_0-1 to d_0+1 where d_0 is the closest bin to the estimated frequency.

The feedback shown in Fig. 1 indicates the need to repeat the operation for each frequency bin, producing the delay-Doppler map of generalized complex correlations.

(e) *Spectrum Windowing.* Two possible window functions are:

$$U(f) = \frac{U_0}{|S(f)|} \quad (5a)$$

$$U(f) = \frac{U_0}{\sqrt{|S(f)|}} \quad (5b)$$

where U_0 is a real constant. Since the GPS signal spectrum falls off with increasing frequency, the inverse magnitude window function of Eq. (5a) acts as a high-pass filter, which tends to emphasize the edge information without affecting the phase information. Since high frequency information decorrelates quickly, it helps to produce a very sharp correlation peak. This operation equalizes the magnitude spectrum, thus keeping the phase-only information.

B. Code Replica Spectrum Filtering

Instead of down-converting the incoming signal from IF to baseband, it is possible to up-convert the code replica from baseband to IF so as to catch up with the incoming signal by accounting for the unknown Doppler shift. This operation is similar to the spectrum translation described above.

(a) *Spectrum Windowing.* Window functions can also be applied to the code replica spectrum as shown in Fig. 1. Two possible window functions are:

$$V(f) = \frac{V_0}{|R(f)|} \quad (6a)$$

$$V(f) = \frac{V_0}{\sqrt{|R(f)|}} \quad (6b)$$

where V_0 is a real constant. It has the same effects as on the incoming signal spectrum described above for Eq. (5).

(b) *Amplitude Compensated Filtering.* A nonlinear filter can be used to attenuate any dc information near the origin on the frequency axis:

$$V(f) = \begin{cases} \frac{R_0}{|R(f)|^2} & |R(f)| > R_0 \\ 1 & |R(f)| < R_0 \end{cases} \quad (7)$$

where R_0 is a positive constant selected to maximize the signal to noise ratio [8].

C. Correlation Spectrum Filtering and Feedback

A window function can be applied to the correlation spectrum. This will shape the correlation function after the inverse Fourier transform is taken. Design goals include (1) reducing the sidelobe level, (2) maximizing the correlation peak, and (3) narrowing the mainlobe. These goals typically are not compatible to each other. For example, reducing the sidelobe level comes at a price of enlarging the mainlobe.

Another useful operation is to evaluate the correlation function at a desired code lag. In the acquisition mode, since the code phase is unknown, a large interval of code phase (timing) uncertainty is searched. However, once in the tracking mode, the estimated code phase and its uncertainty can be used to determine code lags where the correlation function needs to be evaluated [14]. The feedback shown in Fig. 1 indicates the number and location of the code lags to evaluate.

III. SYMMETRIC PHASE-ONLY MATCHED FILTER (SPOMF) FEATURES

Given the possible ways to filter the incoming signal, replica, and correlation spectra jointly or independently, we consider four cases of particular interest to the GFDC implementation.

(a) *Correlation Function*. In the first case where $U(f) = V(f) = W(f) = 1$, the generalized correlation spectrum becomes:

$$C(f) = S(f)R^*(f) \quad (8a)$$

$$c(t) = \text{IFFT}\{C(f)\} \quad (8b)$$

where the superscription * stands for complex conjugate.

Eq. (8a) is the conventional correlation spectrum and Eq. (8b) is just the FFT-implemented cross-correlation.

(b) *Signal Channel Transfer Function/Impulse Response*. In the second case where $U(f) = V(f) = 1/|R(f)|$ and $W(f) = 1$, the generalized correlation spectrum becomes:

$$C(f) = \frac{S(f)R^*(f)}{|R(f)|^2} = \frac{S(f)}{R(f)} \quad (9a)$$

$$h(t) = \text{IFFT}\{C(f)\} \quad (9b)$$

Eq. (9a) is the GPS signal channel transfer function and Eq. (9b) is the corresponding impulse response.

Although $V(f) = 1/|R(f)|$ effectively extracts the phase-only information from the replica $R(f)$, $U(f)$ may fail to do so because $S(f)$ generally differs from $R(f)$ due to residual Doppler and noise. By consequence, some spectral spikes show up near multiples of chipping rate where noise is known to dominate. To suppress such noise amplification effects, spectral filtering such as zone-zeroing and individual excision can be applied [17, 18].

(c) *Phase-Only Matched Filter (POMF)*. In the third case where $U(f) = 1$, $V(f) = 1/|R(f)|$, and $W(f) = 1$ (or equivalently, $U(f) = V(f) = |R(f)|^{-1/2}$ and $W(f) = 1$), the generalized correlation spectrum becomes:

$$C(f) = \frac{S(f)R^*(f)}{|R(f)|} \quad (10)$$

In this operation, the incoming signal is correlated with a phase-only version of the replica, hence the name “phase-only.” Since the incoming signal may differ from the replica greatly in magnitude, the POMF may perform poorly in some cases.

Eq. (7) can be viewed as a combination of the impulse response of Eq. (9) and the phase only matched filter of Eq. (10) as a function of the replica amplitude.

(d) *Symmetric Phase-Only Matched Filter (SPOMF)*. In the final case where $U(f) = 1/|S(f)|$, $V(f) = 1/|R(f)|$, and $W(f) = 1$, the generalized correlation spectrum becomes:

$$C(f) = \frac{S(f)R^*(f)}{|S(f)||R(f)|} \quad (11)$$

A variation of this filter is to normalize the incoming signal and the replica spectra with the square root of their respective magnitude spectrum, that is, $U(f) = |S(f)|^{-1/2}$, $V(f) = |R(f)|^{-1/2}$, and $W(f) = 1$.

In Eq. (11), $S(f)/|S(f)|$ removes the magnitude information from the incoming signal spectrum and retains only the phase information. Similarly, $R(f)/|R(f)|$ removes the magnitude information from the code replica spectrum and retains only the phase information. The equalization is applied to both the incoming signal and replica, hence the name “symmetric.” Since both the incoming signal and replica amplitude contents are involved in weighting, the spectral filtering is therefore “balanced” [Wernet, 2005].

Ideally, a flat infinite spectrum produces a Dirac delta function in the time domain. By eliminating the shape information from the two input spectra, the phase only filtering (attenuating the magnitude information and accentuating the phase information in the frequency domain) can sharpen the correlation peak in the time domain.

The importance of phase in signals has been recognized for many applications in which a signal can be recovered completely or in part from knowledge of its phase alone. In a number of contexts [9], the Fourier transform’s phase data contain more of the “important” information than the Fourier transform’s magnitude data. In a sense, the phase reflects the location of “events” more than magnitude whereas the magnitude contains information more relevant to the size and shape of an object. The time shift property is an example: a translation in position (time or space) of a signal has no effect on the Fourier transform magnitude but only affects the phase by adding a linear phase term.

Conditions are given in [9] under which the spectral magnitude is uniquely specified to within a scaling factor by its phase function. For example, the log magnitude of the Fourier transform is the Hilbert transform of the phase of a signal with all poles and zeros lying only in the left half or only in the right half of the s-plane (the minimum- or maximum-phase condition).

Since the autocorrelation function of phase-only signals is always an impulse, this feature has been used in designing methods for image registration and recognition [2] and digital image velocimetry [13].

IV. SIMULATION RESULTS AND ANALYSIS

Three simulation examples are provided to illustrate the use of SPOMF for processing GPS signals (BPSK and BOC-codes) and in particular its superior multipath performance.

A. Bandwidth Limiting vs. Phase-Only

It is well known that both the GPS signal and the RF front-end of a GPS receiver have limited bandwidth, too. The effect

of such a bandwidth limitation is a rounding of the correlation function at the peak. To see this, the following simulation is conducted in which the C/A-code of GPS SVN10 is chosen and the sampling rate is set at $f_s = 5$ MHz with an equivalent correlator spacing of 0.2046 chips. A 5th-order Butterworth low-pass filter is used for band-limiting filtering with its corner frequency set at 1.023 MHz.

Fig. 2 shows the first 150 samples of the ideal C/A-code (blue) in comparison to the bandpass filtered code (green). For the filtered codes, there are ringings after each transition and the filtered code sequence seems to be shifted in time due to the group delay impacted by the lowpass filtering. The ringing goes away and transitions of first order appear if the corner frequency is set smaller (or the transition band is set larger). Fig. 3 shows the ideal code amplitude spectrum (blue) and the filtered code spectrum (green). The latter is effectively band-limited around 1.023 MHz as designed. Fig. 4 shows the ideal correlation function (blue) of a triangular shape and the filtered correlation function (green), which is smaller in amplitude and is rounded up at the correlation peak. Fig. 5 compares the autocorrelation functions of the ideal PRN code (blue), the filtered code (green), the phase-only version of the ideal code (red), and the phase-only version of the filtered code (cyan). The autocorrelation functions of the two phase-only codes have the same shape, which is much narrower and of smaller noise floor than the two originals.

To visualize a PRN code and its phase-only version, the following simulations are conducted first for a BPSK code and then for a BOC code. Fig. 6 shows the GPS C/A-code sampled at 5 MHz and its phase-only version (normalized to unity amplitude). Their normalized autocorrelation functions are shown in Fig. 7. Similarly, Fig. 8 shows the GPS C/A-code sampled at 10 MHz and its phase-only version (normalized) with their normalized autocorrelation functions in Fig. 9.

Fig. 10 shows a BOC(10, 5)-code sampled at 50 MHz and its phase-only version (normalized to the unity amplitude). Their normalized autocorrelation functions are shown in Fig. 11. Similarly, Fig. 12 shows the same BOC code sampled at 100 MHz and its normalized phase-only version with their normalized autocorrelation functions in Fig. 13.

It is interesting to see that the phase-only version of both the BPSK and BOC codes produces a pair of spikes of opposite directions at a transition. The signal returns to zero during quiescent periods with small variations. The effect is more pronounced when the sampling rate is higher. This indicates that the phase-only waveform possesses the property of some specially designed codes such as double delta, strobe, pulsed aperture, and gated correlator that are employed in the state of the art conventional GPS receivers and are known to reduce multipath errors [21, 22, 23].

B. BOC Modulation Codes

In this simulation, we use the following method to construct a BOC(10, 5)-code similar to the M-code. It is easy to generate the subcarrier with a square wave at the fundamental frequency of 10.23 MHz (an equivalent chipping

rate is 20.46 Mcps). We use the CL component of the L2C code (which is 1.5 s long) as the PRN code at 5.115 Mcps (another choice is the P-code). The correlation and spectral properties of these surrogate codes may not be as good as the actual M-code, which is infinitely long and cryptographic, thus representing a worse case of signal conditions.

The PRN-code and the square wave are modulo-2 added, multiplied with a complex exponential to simulate the residual carrier plus complex Gaussian white noise. The resulting signal at the baseband is then sampled at 50 MHz and passed through a 5th-order Butterworth low-pass filter with its corner frequency set at 12 MHz. Fig. 14 shows the amplitude spectrum of the code sequence sampled at 50 MHz. Fig. 15 shows the spectrum after the signal is lowpass-filtered within 12 MHz.

In this simulation, the residual Doppler error is set to be 200 Hz. The code phase error is $\frac{1}{2}$ the sampling interval (i.e., between two samples). The initial carrier phase is drawn uniformly from $[0, 2\pi)$. A complex Gaussian noise of unity variance is added. The signal amplitude is adjusted to simulate the desired SNR level according to:

$$A = (T_i 10^{\frac{C/N_0}{10}})^{\frac{1}{2}} \quad (12)$$

where $T_i = 0.001$ s and $C/N_0 = 30$ dB-Hz for this simulation. The resulting SNR is 1 (in ratio).

A segment of 1 ms code is taken from a long sequence of the simulated M-code starting from the 1000th chip as the replica (the true peak location is at 2444.3). Fig. 16 shows a portion of the correlation where the peak value is about 31200 and the noise floor peak is about 1900. The peak to noise peak ratio is 16.42 (or 24.31 dB).

The ideal correlation value is 50000. However, the code phase error of $\frac{1}{2}$ the sampling interval (0.2046 chips) reduces it by a factor of 0.7954. The Doppler error of 200 Hz (relative to the 1 ms integration interval) introduces a loss factor less than 0.92. The 12 MHz lowpass filter introduces a loss factor less than 0.86. The practical peak value is around 31466, which is close to what we can observe from Figs. 16 and 17 (the absolute peak value around 31200).

It is also clear from Figs. 16 and 17 that the BOC modulation has sidelobes in addition to the main peak. This is problematic for conventional tracking loops with the risk of locking onto a secondary peak if the correlator spacing is small, less than a $\frac{1}{4}$ of the subcarrier wavelength for instance.

Fig. 17 shows the real and imaginary components of the complex correlation. In the acquisition mode, carrier phase and frequency tracking are not yet applied. It is not dominated by the real component as is caused by the Doppler frequency error. For this particular segment of data, the real and imaginary components have about the same power.

Figs. 18 and 19 compare the conventional (green) correlation with the impulse response (red) and the symmetric phase-only (blue) correlation. As explained before, similar to the phase-only correlation in Eq. (10), the impulse response in Eq. (9) equalizes the replica spectrum. Although producing very narrow peak, it tends to develop large sidelobes as

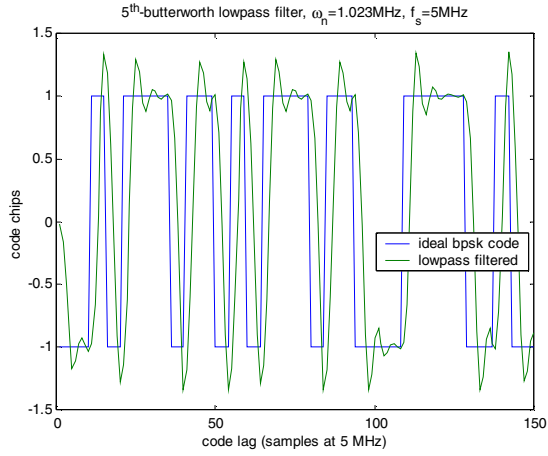


Fig. 2. Ideal PRN vs. Lowpass Filtered Code

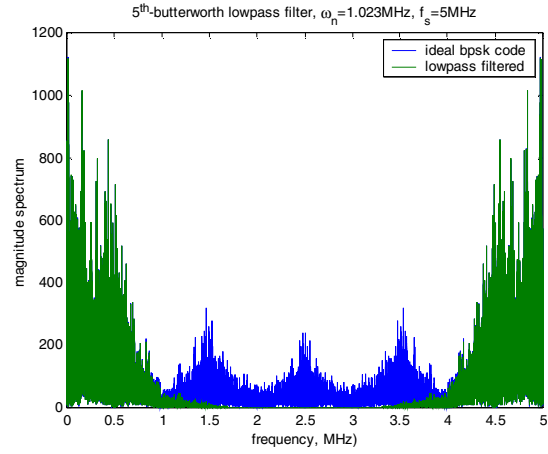


Fig. 3. Ideal PRN vs. Lowpass Filtered Spectra

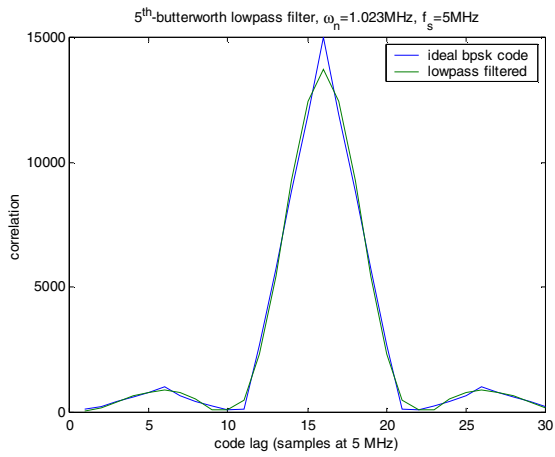


Fig. 4. Ideal PRN vs. Lowpass Filtered Autocorrelations

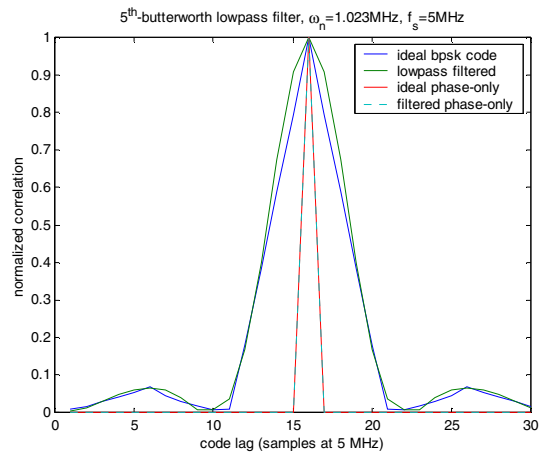


Fig. 5. Conventional vs. Phase-Only Autocorrelations

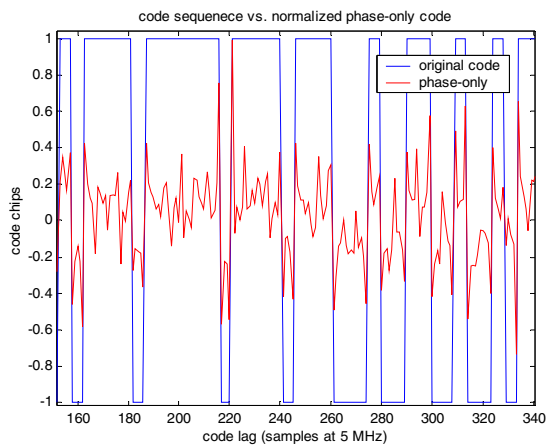


Fig.6. Ideal PRN vs. Phase-Only Codes

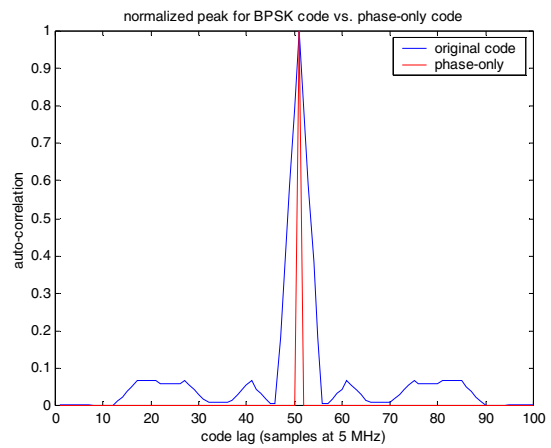


Fig.7. Ideal vs. Phase-Only Autocorrelations

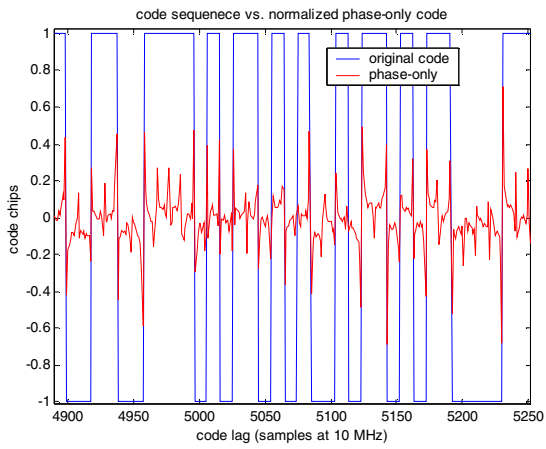


Fig. 8. Ideal PRN vs. Phase-Only Codes

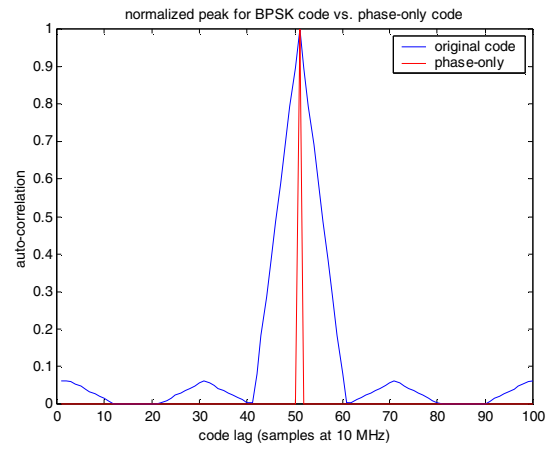


Fig.9. Ideal vs. Phase-Only Autocorrelations

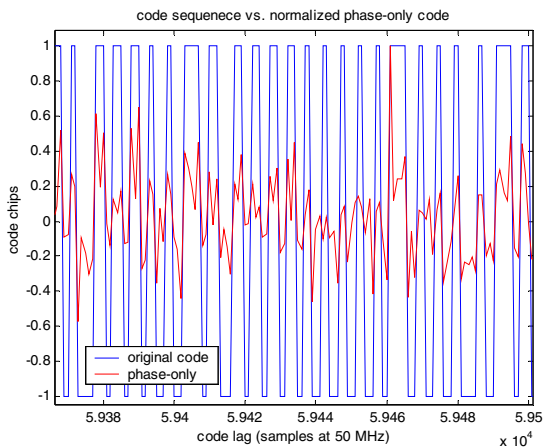


Fig. 10. Ideal PRN vs. Phase-Only Codes

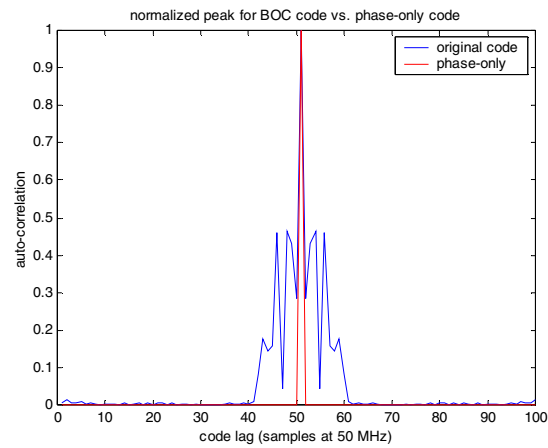


Fig. 11. Ideal vs. Phase-Only Autocorrelations

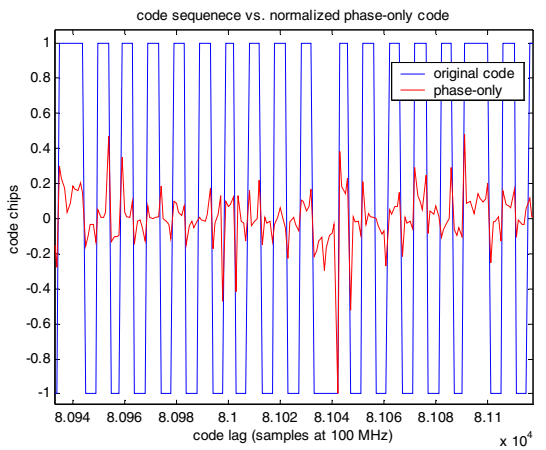


Fig. 12. Ideal BOC(10, 5) vs. Phase-Only Codes

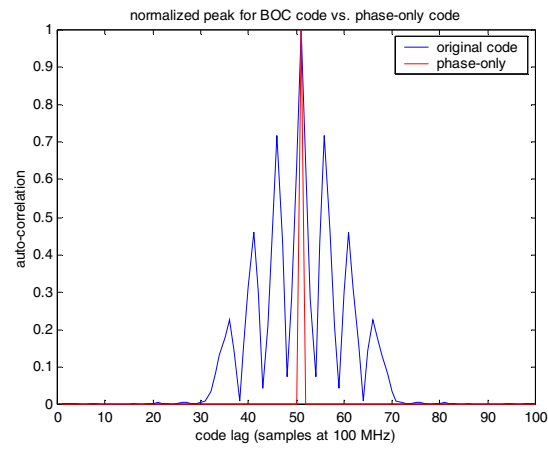


Fig. 13. Ideal vs. Phase-Only Autocorrelations

shown in Fig. 18. Spectral filters such as zone zeroing and individual excision have been used to reduce the noise floor [18].

The symmetric phase-only matched filter equalizes both the incoming signal and replica spectra. As such, it not only produces a peak as narrow as the phase-only matched filter, but also keeps the noise floor as low as the conventional correlator as shown in Fig. 19.

C. BPSK Modulation Codes

The multipath performance of the SPOMF is demonstrated in the following example with a BPSK code (the GPS SVN10 C/A-code). The signal ms boundary is ahead of the first sample by $0.45T_s$. One multipath component is considered with $\tau_l = 0.5$ chips (2.4438 samples) and $\alpha_l = 0.2$.

We first compare the signal channel impulse response with the conventional correlation function in Figs. 20 and 21 for two spectral filtering methods, namely, zone zeroing and individual excision [17, 18]. The top plots in Figs. 20 and 21 correspond to the case where the incoming signal contains direct signal and noise only without multipath whereas the bottom plots of Figs. 20 and 21 contain the direct signal, noise, and multipath.

It is clear that the peak of the impulse response function is narrower than that of the correlation function. The latter is about $2 \times 5 / 1.023 = 9.7752$ samples wide whereas the former is about 3 samples wide. This has significant ramifications in multipath performance.

For multipath delays larger than one sampling interval, which is 0.2 chips in this simulation, the individual multipath components can be resolved, thus not causing errors to the direct signal. For those within 0.2 chips, the multipath affects the correlation values at adjacent sampling points. Since the direct signal is stronger, an interpolation can be used to find the underlying peak location.

In Fig. 22, the multipath delay is varied from 0.05 to 1.5 chips in step of 0.1 chips. In each case we show the performance of four different methods. The four methods are: (1) quadratic fitting to the correlation function (blue), (2) *sinc* fitting to the impulse response without filtering (green), (3) *sinc* fitting to the impulse response with zone zeroing (red), and (4) *sinc* fitting to the impulse response with individual excision (cyan).

The correlation function interpolated estimate without multipath mitigation follows closely the multipath error envelope, which is determined by the correlation spacing $d = 0.2$ chips and multipath strength $\alpha_l = 0.2$ (i.e., $d\alpha_l = 0.04$ or 12 m).

The two spectral filtering methods perform consistently better than the one without spectral filtering. Between the two spectral filtering methods, the individual excision method seems marginally better than the zone zeroing. The data shown in the figures are taken from sample runs, each with 1 ms worth of data samples. Averaging over many runs may smooth out variations in the curves.

In Fig. 23, the delay estimation errors of the symmetric phase-only matched filter are compared with those of two spectral filtered impulse responses. Once again, the

individual excision method marginally performs better than the zone zeroing. The symmetric phase-only matched filter performs best.

In addition to the sample behavior shown above, we also conducted Monte Carlo runs. The root mean squared (RMS) values of the errors in estimating the direct signal delay (τ_0) as a function of the multipath signal delay (τ_l) are shown in Figs. 24 and 25 for $C/N_0 = 40$ dB-Hz and 30 dB-Hz, respectively. The multipath strength is fixed at $\alpha_l = 0.2$.

In each figure, there are three pairs of curves, representing three different estimation techniques. Each pair consists of two types of signals, namely, (1) direct signal plus noise (s + n) and (2) direct signal plus noise plus multipath signal (s + n + m). The first delay estimation technique is the normalized early minus late delay error discriminator applied to the correlation power. With the correlation spacing $d = 0.2046$ chips and the multipath strength $\alpha_l = 0.2$, the expected error is on the order of $d\alpha_l = 0.04$ or 12.28 m.

The second technique is the fitting of a *sinc*-function to the impulse response peak after individual excision of spectral spikes is done in the frequency domain. The third technique is the fitting of a *sinc*-function to the symmetric phase-only matching peak.

Each Monte Carlo simulation consists of 100 runs. For each run, the initial carrier phase and noise are drawn randomly from their respective distributions. However, the random values are kept the same when the multipath signal delay is varied from 0.1 to 1.4 chips in the step of 0.1 chips. This helps explaining why the delay estimation errors for the three “signal plus noise” cases (green, cyan, and yellow, respectively) remain constant in the figures.

While a conventional correlation-based delay estimation technique produces the typical multipath error envelope even when the SNR is high (see the blue curve of Fig. 24), both the impulse response (red) and symmetric phase-only matching (purple) techniques perform similarly with an almost flat error level, indicating the insensitivity to multipath. Their error level is slightly higher than the “signal plus noise” cases. As expected, they all attain the same level of performance when the multipath delay goes beyond $(1+d)$ chips after which the multipath does not interfere with the direct signal and the noise dominates.

When the SNR is low, all “signal plus noise” curves are raised in their error level. The impulse response (red) and symmetric phase-only matching (purple) techniques start to behave differently. Both the techniques are still effective in suppressing the multipath effects because their “signal plus noise plus multipath” curves (red and purple) stick rather closely to the “signal plus noise” curves (cyan and yellow). However, the impulse response (red and cyan) technique experiences a noise amplification effect as observed in the sample behavior. The error level (red and cyan) is higher than the conventional correlation noise floor (green).

In contrast, the symmetric phase-only matching (purple and yellow) technique maintains an almost flat multipath error level, which is even slightly lower than the conventional correlation noise floor (green). This may be explained by the

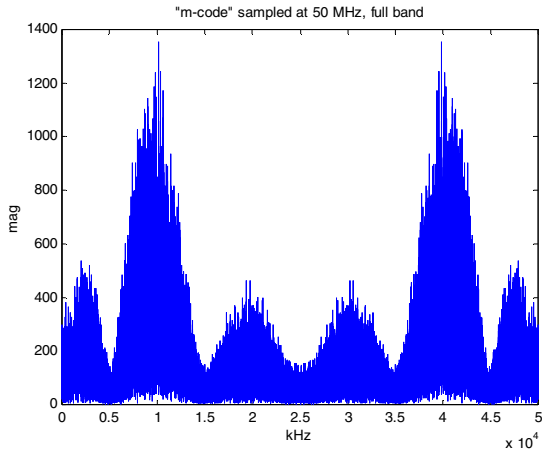


Fig. 14. M-Code Sampled at 50 MHz

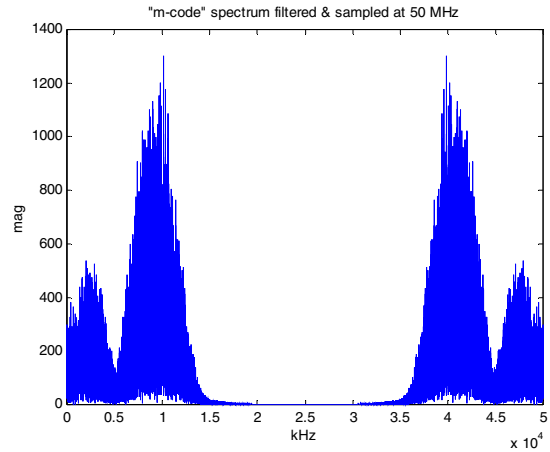


Fig. 15. Spectrum after Filtering

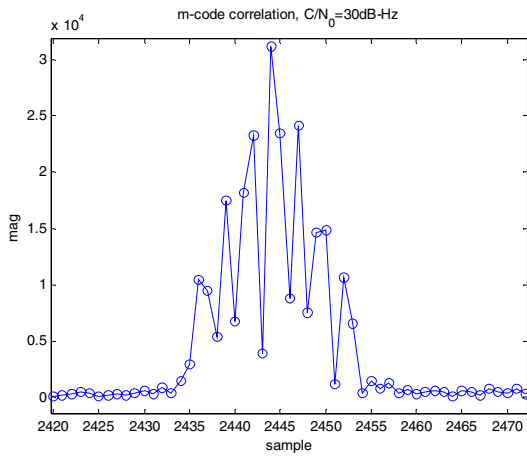


Fig. 16. A Portion of Correlation at 50 MHz

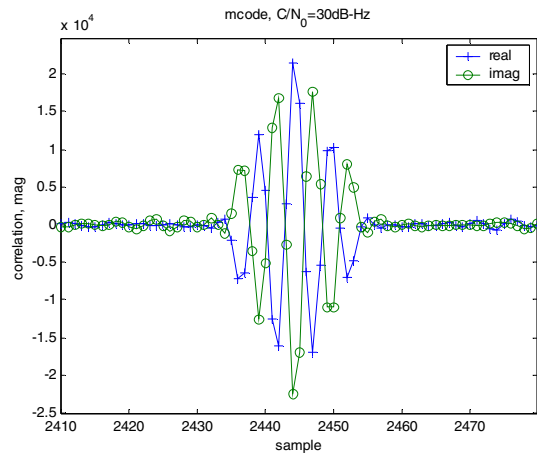


Fig. 17. Real and Imaginary Parts of Correlation (50 MHz)

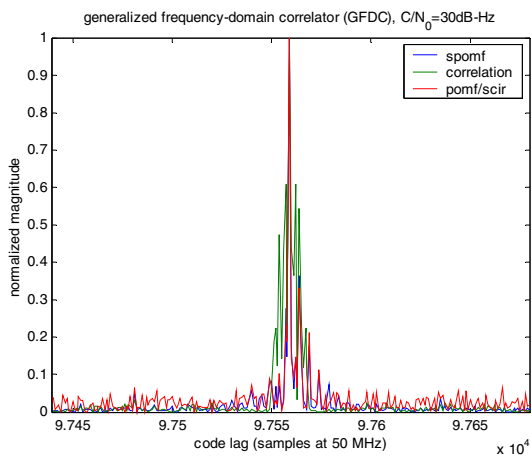


Fig. 18. Conventional vs. Phase-Only Correlations

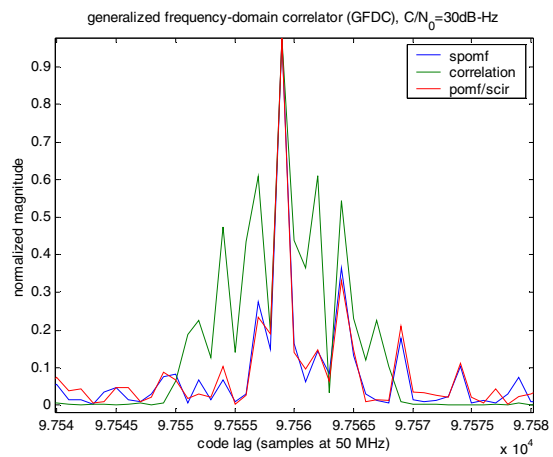


Fig. 19. Conventional vs. Phase-Only Correlations

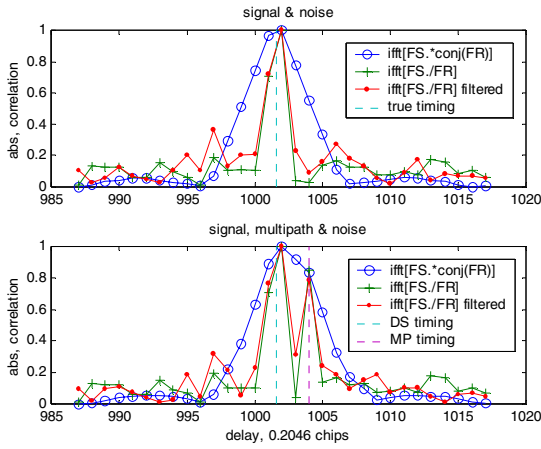


Fig. 20. Ideal vs. Phase-Only Correlation (Impulse Response with Zone Zeroing)

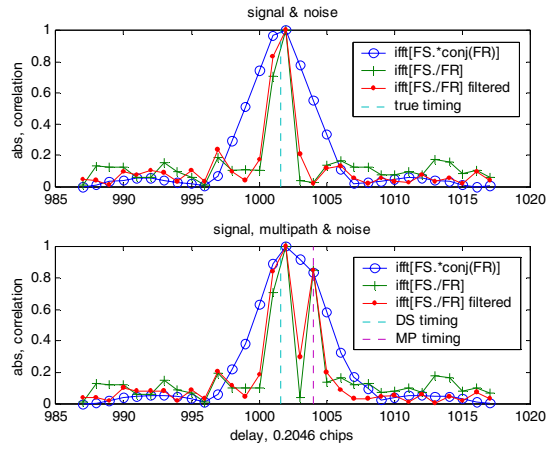


Fig. 21. Ideal vs. Phase-Only Correlation (Impulse Response with Individual Excision)

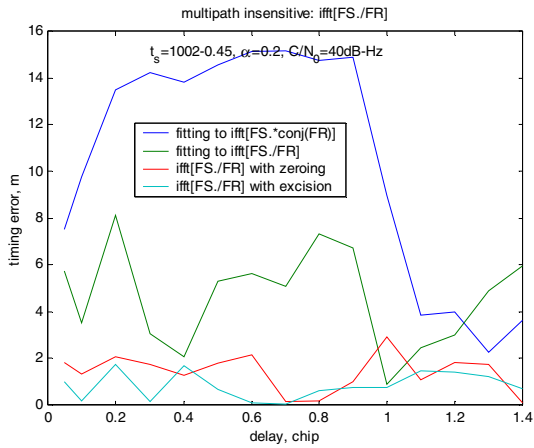


Fig. 22. Multipath Error Envelopes for Ideal vs. Phase-Only Correlation with Different Filtering (Impulse Response $\alpha_1 = 0.2$, $C/N_0 = 30$ dB-Hz)

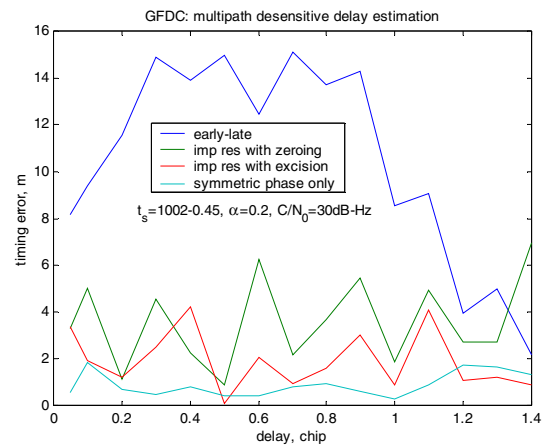


Fig. 23. Multipath Error Envelope for Filtered Phase-Only vs. Symmetric Phase Only Correlation ($\alpha_1 = 0.2$, $C/N_0 = 30$ dB-Hz)

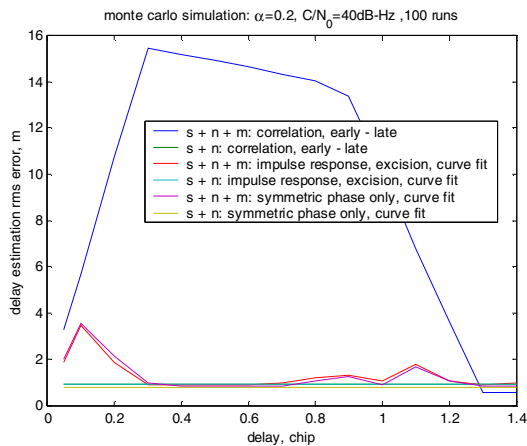


Fig. 24. Delay Estimation Error RMS ($\alpha_1 = 0.2$, $C/N_0 = 40$ dB-Hz)

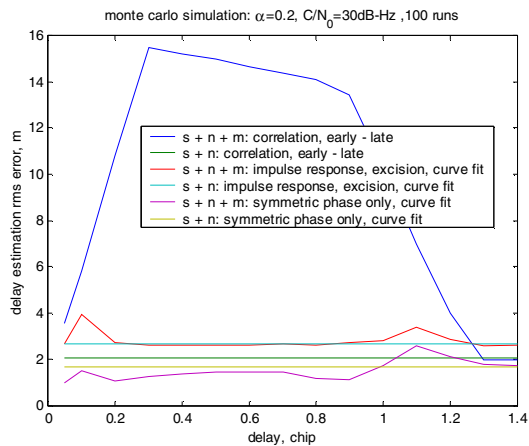


Fig. 25. Delay Estimation Error RMS ($\alpha_1 = 0.2$, $C/N_0 = 30$ dB-Hz)

fact that the slope of SPOMF peak is steeper than that of the conventional correlators, thus having smaller noise variance. Overall, the simulation results indicated the consistency and superiority of the SPOMF technology versus conventional correlators.

V. CONCLUSIONS

In this paper, we set forth a generalized frequency-domain correlator (GFDC) as an efficient computing engine for a new generation of software GNSS receivers. With its inherent flexibility, the GFDC can be programmed to provide the most suitable form of correlation when operating in both the acquisition and tracking modes. In acquisition, the desired correlation is of a wide base, which can be obtained by FFT-implemented conventional correlation for the BPSK modulation or for a single sideband if the BOC modulation. In tracking, the desired correlation is of a narrow base, which is achieved with the symmetric phase-only matched filtering (SPOMF). The same operation is applicable to both the BPSK and BOC codes. With spectral filtering and feedback closure, the GFDC realizes a seamless transition from acquisition and tracking.

Simulation results showed the SPOMF indeed provided a very sharp correlation peak that was more accurate in timing and less sensitive to multipath. The SPOMF has been applied to real GPS data that are known to contain multipath. The initial test results will be presented in [20] together with analysis of such effects as signal bandwidth and code replica filtering.

REFERENCES

- [1] J.W. Betz, "Binary Offset Carrier Modulation for Radionavigation," *Navigation: The Journal of the Institute of Navigation*, 48(4), Winter 2001-2002.
- [2] Q.S. Chen, M. Defrise, and F. Deconick, "Symmetric Phase-Only Matched Filtering of Fourier-Mellin Transforms for Image Registration and Recognition," *IEEE Trans. Pattern Analysis and Machine Intelligence*, 16(12), Dec. 1994.
- [3] P. Fine and W. Wilson, "Tracking Algorithm for GPS Offset Carrier Signals," *ION-NTM'99*, January 1999.
- [4] J.C. Hassab and R.E. Boucher, "Optimum Estimation of Time Delay By A Generalized Correlator," *IEEE Trans. Acoust. Speech Signal Process.*, 27, 1979.
- [5] E.D. Kaplan (ed.), *Understanding GPS: Principles and Applications*, Artech House Publishers, Norwood, MA, 1996.
- [6] C.H. Knapp and G.C. Carter, "The Generalized Correlation Method for Estimation of Time Delay," *IEEE Trans. Acoust. Speech Signal Process.*, 24, 1976.
- [7] P. Misra and P. Enge, *Global Positioning System, Signals, Measurements, and Performance*, Ganga-Jamuna Press, 2001.
- [8] G.G. Mu and X.M. Wang, and Z.Q. Wang, "Amplitude Compensated Matched Filtering," *Applied Optics*, 69, 1981.
- [9] A.V. Oppenheim and J.S. Lim, "The Importance of Phase in Signals," *Proceedings of the IEEE*, 69(5), May 1981.
- [10] B.W. Parkinson, and J.J. Spilker Jr. (eds.), *Global Positioning System: Theory and Applications*, AIAA, 1996.
- [11] B. Peterson, R.J. Hartnett, R. Friedler, and A. Nebrich, "Frequency Domain Techniques for Fast GPS Acquisition and Interference Detection/Rejection," *Navigation: J. of the Institute of Navigation*, 43(3), Fall 1996.
- [12] J.B.Y. Tsui, *Fundamentals of Global Positioning System Receivers - A Software Approach*, John Wiley & Sons, Inc., 2000.
- [13] M.P. Wernet, "Symmetric Phase Only Filtering: A New Paradigm for DPV Data Processing," *Measurement Science and Technology*, 16, 2005.
- [14] C. Yang, "Tracking of GPS Code Phase and Carrier Frequency in the Frequency Domain," *Proc. of ION-GPS/GNSS'03*, Sept. 2003.
- [15] C. Yang, *Novel Global Navigation Satellite System (GNSS) Receivers Based on Satellite Signal Channel Impulse Response*, U.S. Patent-Pending (S/N: 11/188,258), Feb. 2005a.
- [16] C. Yang, "Frequency-Domain GPS Receiver for Modernization GPS Signals via Full-Band Multi-Code Processing," *ION-GNSS'05*, September 2005b.
- [17] C. Yang and M. Miller, "Novel GNSS Receiver Design Based on Satellite Signal Channel Transfer Function/Impulse Response," *ION-GNSS'05*, September 2005.
- [18] C. Yang and A. Porter, "Multipath Desensitized Delay Estimation with GPS Signal Channel Transfer Function Filtering," *ION-AM'05*, June 2005.
- [19] C. Yang, J. Vasquez, and J. Chaffee, "Frequency-Domain Doppler Search and Jam-Suppression for Fast Direct P(Y)-Code Acquisition," *Proc. of ION-GPS'99*, Sept. 1999.
- [20] C. Yang, M. Miller, T. Nguyen, and D. Akos, "Generalized Frequency-Domain Correlator: Preliminary Test Results and Analysis," To Be Submitted to *ION-GNSS'06*, September 2006.
- [21] L. Garin and J.M. Rousseau, "Enhanced Strobe Correlator Multipath Rejection for Code & Carrier," *ION-GNSS'97*, September 1997.
- [22] S.M. Kanekal and M.S. Braasch, "Multipath Mitigation with Gated Signal Technique," *Proc. of ION-AM'98*, June 1998.
- [23] V. Veitsel, A. Zhdanov, and M. Zhodzishsky, "The Mitigation of Multipath Errors by Strobe Correlators in GPS/GLONASS Receivers," *GPS Solution*, 2(2), Fall 1998..